Targeting cell adhesion molecules with nanoparticles using *in vivo* and flow-based *in vitro* models of atherosclerosis

Khosrow Khodabandehlou*, Jacqueline J Masehi-Lano*, Christopher Poon*, Jonathan Wang and Eun Ji Chung

Department of Biomedical Engineering, University of Southern California, Los Angeles, CA 90089, USA
*These authors contributed equally to the work.
Corresponding author: Eun Ji Chung. Email: eunchung@usc.edu

Impact statement

As atherosclerosis remains the leading cause of death, there is an urgent need to develop better tools for treatment of the disease. The ability to improve current treatments relies on enhancing the accuracy of *in vitro* and *in vivo* atherosclerotic models. While *in vivo* models provide all the relevant testing parameters, variability between animals and among models used is a barrier to reproducible results and comparability of NP efficacy. *In vitro* cultures isolate cells into microenvironments that fail to take into account flow separation and shear stress, which are characteristics of atherosclerotic lesions. Flow-based *in vitro* models provide more physiologically relevant platforms, bridging the gap between *in vivo* and 2D *in vitro* models. This is the first review that presents recent advances regarding endothelial cell-targeting using adhesion molecules in light of *in vivo* and flow-based *in vitro* models, providing insights for future development of optimal strategies against atherosclerosis.

Abstract

Atherosclerosis is a leading cause of death worldwide; in addition to lipid dysfunction, chronic arterial wall inflammation is a key component of atherosclerosis. Techniques that target cell adhesion molecules, which are overexpressed during inflammation, are effective methods to detect and treat atherosclerosis. Specifically, research groups have identified vascular cell adhesion molecule-1, intercellular adhesion molecule-1, platelet endothelial cell adhesion molecule, and selectins (E-selectin and P-selectin) as correlated to atherogenesis. In this review, we discuss recent strategies both *in vivo* and *in vitro* that target cell adhesion molecules. First, we discuss peptide-based and antibody (Ab)-based nanoparticles utilized *in vivo* for diagnostic, therapeutic, and theranostic applications. Second, we discuss flow-based *in vitro* models that serve to reduce the traditional disadvantages of *in vivo* studies such as variability, time to develop the disease, and ethical burden, but preserve physiological relevance. The knowledge gained from these targeting studies can be translated into clinical solutions for improved detection, prevention, and treatment of atherosclerosis.

Keywords: Cell adhesion molecules, atherosclerosis, nanoparticles, flow-based models, endothelial cells, targeting

***Experimental Biology and Medicine* 2017; 242: 799–812. DOI: 10.1177/1535370217693116**

Introduction

Cardiovascular disease (CVD) is the leading cause of death in the USA, with approximately 801,000 deaths each year.[1] The most common type of CVD is atherosclerosis, which accounts for 68% of CVD deaths.[2] Atherosclerosis is a degenerative disease that is characterized by the irregularity of lipid metabolism, endothelial dysfunction, and the buildup of rupture-prone plaques, resulting in acute coronary blockage syndromes and/or sudden cardiac arrest.[3,4] A prominent feature of atherosclerosis is inflammation of the endothelium, which instigates the influx of monocytes to the plaque, driving plaque thickening and rupture.[5,6] Thus, targeting inflamed endothelia has emerged as a therapeutic strategy against atherosclerosis.

The onset of atherosclerotic plaques begins with the accumulation of low-density lipoproteins (LDLs) in the subendothelium.[7,8] Endothelial cells (ECs) are activated to express leukocyte adhesion molecules that result in monocyte recruitment, attachment, and differentiation into macrophages. These macrophages eventually produce enzymes that degrade the extracellular matrix and cause plaque rupture.[9,10] The ECs in these regions respond through mechanosensors, which transduce the local flow shear stress into changes in levels of gene expression.[11] For instance, activated ECs begin to overexpress cell adhesion molecules (CAMs), such as vascular cell adhesion molecule-1 (VCAM-1), intercellular adhesion molecule-1 (ICAM-1), platelet endothelial cell adhesion molecule

(PECAM-1), and selectins (E-selectin and P-selectin) on their surfaces.

There are two major weaknesses in current treatments that prevent conventional small molecule drugs from optimal effectiveness against atherosclerosis: (1) their short blood circulation time and (2) their inability to select for diseased tissue. Nanoparticles (NPs) offer numerous advantages over traditional molecules, including high payloads, tunable sizes, tailorable surface properties, controllable drug kinetics, and improved pharmacokinetics.[12–18] Many NP-based platforms with the ability to target plaques, the hallmark of atherosclerosis, have thus been developed as a novel means to enhance diagnostic sensitivity and therapeutic efficacy.[19–22]

Interactions between NPs and their local environments are dependent on both size and surface properties. Because of their small size (10–200 nm in diameter), NPs can penetrate through ''leaky'' regions of inflamed vasculature, which is known to be part of the enhanced permeability and retention (EPR) effect.[23] When the charge of NP surface is highly positive or negative, clearance by the mononuclear phagocytic system (MPS) macrophages is significantly enhanced. In order to stabilize particles against rapid decomposition in circulation, research groups have encapsulated them within a lipid layer containing water-soluble polymers such as polyethylene glycol (PEG).[24] This coating shields the NP from the immune system, prevents degradation, and increases circulation time to improve drug accumulation and controlled drug release. Furthermore, small molecules, dyes, and targeting moieties can be encapsulated inside or conjugated to the surface of NPs.[25] Targeting moieties, which include peptides, antibodies (Abs), integrin, and endothelial-specific ligands, can drive NPs to localize at the desired site and bind to molecules or receptors expressed on the cell surface.[26] The high surface-to-volume ratio of NPs makes them optimal for conjugating therapeutics or targeting ligands onto their surfaces for enhanced efficacy and avidity. Nanoparticles can also carry drug payloads in their cores, which has been shown to promote therapeutic effectiveness and reduce side effects by improving pharmacokinetics.[17,27–29]

Prior reviews have provided a biological understanding of how CAMs play a critical role in the development of atherosclerosis and plaque rupture, but only a few have considered NPs targeting CAMs and their testing in both *in vivo* and *in vitro* atherosclerotic models.[30–33] The treatment of atherosclerosis is often limited by the lack of understanding regarding the interplay between the NP and the endothelium. *In vivo* models provide a platform that includes all the parameters in a physiologically functional system, which usually suggests clinical relevance. However, the ethical issues and high costs associated with the use of animals and the inherent variable nature between individual specimens are barriers to repeatable results and comparability of NP efficacy. At the other end of the spectrum are highly controlled 2D cell cultures, which force cells into isolation and do not provide a physiologically relevant microenvironment. *In vitro* flow models can close the gap between 2D cell culture and animal experiments, providing additional parameters such as shear stress, 3D architecture, and co-culture conditions. In this review, current targeted strategies using NPs are reviewed, focusing on targeting moieties that enable NP localization to activated ECs expressing VCAM-1 as well as other major CAMs. We first discuss recent developments of diagnostic and therapeutic NPs targeting ECs using peptides and Abs in *in vivo* models (Table 1). The second half of this review focuses on the *in vitro* flow models that have been specifically developed for evaluating the targeting efficiency of particles to the endothelium using CAMs, as well as models investigating CAM expression and leukocyte recruitment in response to disturbed flow conditions.

Table 1 Nanoparticles targeting cell adhesion cells for *in vivo* diagnostic, therapeutic, and theranostic applications in atherosclerotic-related diseases

Targets	Targeting moieties	Treatments	Particle types	References
VCAM-1	VHSPNKK Peptide	Diagnostics	Magnetofluorescent	38
	VHPKQHR Peptide	Diagnostics	Magnetofluorescent	39
	VHPKQHR Peptide	Diagnostics	Micelle	40
	VLTTGLPALISWIKRKRQQ Peptide	Diagnostics	Perfluorocarbon Cored Nanocarrier	41
	NNSKSHT Peptide	Diagnostics	SPIO	42,43
	VHPKQHRAEEAK Peptide	Diagnostics	Tobacco Mosaic Virus	44
	C*NNSKSHTC*C Peptide	Diagnostics	Micelle	45
	VHPK Peptide	Therapeutics	Cationic Lipoparticle	46
	VHPKQHRGGSKGC Peptide	Therapeutics	Liposome	47
	VHSPNKK	Theranostics	Simian Virus 40	49
	Ab(M/K-2.7)	Diagnostics	Iron Oxide	54
	Ab(429)	Diagnostics	Gold Nanoshell	55
	Nanobodies	Diagnostics	Nanobody	56
	Ab	Therapeutics	Liposome	57
PECAM-1	Ab	Therapeutics	Polymer Nanocarrier	58
ICAM-1	LFA-1 Integrin	Imaging	SPIO	59
	Ab(R6.5)	Therapeutics	Antibody carrier	60

In vivo models and CAMs expression

Peptide-based nanomaterials for targeting VCAM in vivo

VCAM-1 is an adhesion molecule that is overexpressed on the surfaces of inflamed ECs in atherosclerosis.[34,35] VCAM-1 acts as a mediator in the recruitment of monocytes to the plaque.[31] It plays a critical role in the inflammatory process and its expression is often correlated with the progression of atherosclerotic lesions. For these reasons, VCAM-1 expression is a reliable target to consider in the development of several *in vivo* imaging tools and therapies against atherosclerosis. One strategy to incorporate a biomarker for cell-specific binding and localization is by modifying the surface of NPs with peptides. Peptide-based nanomaterials provide greater selectivity than free drugs, therefore limiting the potential off-target side effects generally associated with small molecule targeting.[36] Due to their ability to form secondary structures, such as helices and coils, peptides can be presented on the exterior of the NP for active targeting.[37] In addition, their small size offers enhanced penetration into tissues over whole proteins.[36]

Recent efforts have been directed toward enhancing *in vivo* diagnostic methods to detect vulnerable, atherosclerotic plaques prone to rupturing, which can allow for earlier intervention and may ultimately reduce the numbers of heart attacks and strokes. A number of imaging modalities exist for vulnerable plaque detection, from optical imaging to magnetic resonance imaging (MRI). Kelly *et al.* used phage display to derive the peptide sequence VHSPNKK that could target and be internalized by VCAM-1.[38] This sequence is homologous to the alpha-chain of late antigen (VLA-4), which is expressed by the monocytes and lymphocytes that bind to VCAM-1 on activated EC surfaces. Kelly *et al*. synthesized VHSPNKK-modified magnetofluorescent NPs with superparamagnetic and fluorescent properties to enable evaluation of VCAM-1 expression via fluorescence imaging or MRI. The peptide-conjugated NP successfully targeted VCAM-1-expressing ECs and accumulated in the vessel wall of apolipoprotein E-knockout ($ApoE^{-/-}$) mice. Under fluorescence imaging, the peptide-conjugated NPs exhibited enhanced target-to-background ratios of about 12-fold higher compared to those functionalized with VCAM-1 monoclonal Abs. Moreover, it was demonstrated for the first time that endothelial targets could be detected *in vivo* by MRI without the use of VCAM-1 Abs. Nahrendorf *et al*. developed a second generation of these VCAM-1-targeting magnetofluorescent NPs for the detection of early-stage inflammation in cholesterol-fed $ApoE^{-/-}$ mice. More specifically, the NPs were conjugated to a different linear VCAM-1-targeting peptide, VHPKQHR (VHP), which was shown to exhibit higher cellular internalization for enhanced MRI resolution and optical imaging.[39] Injecting these particles into $ApoE^{-/-}$ mice led to a 77% increased contrast-to-noise ratio between the aortic wall and adjacent blood pool by MRI imaging. Fluorescent images confirmed these results, as the aortic root had a 350% higher plaque target-to-background ratio compared to saline-injected $ApoE^{-/-}$ mice. Mlinar *et al.* also reported conjugating the same peptide discovered by Nahrendorf *et al*. to the surfaces of spherical, self-assembled peptide amphiphile micelles (PAMs). Apart from having targeting capabilities, the PAMs were labeled with the fluorochrome Cy7 to enable particle tracking and fluorescence imaging *in vivo*.[40] After 24 h post injection, these VCAM-1-targeting PAMs were able to differentiate between early- and mid-stage atherosclerotic plaque in $ApoE^{-/-}$ mice (Figure 1). Others have reported using alternative peptides to target VCAM-1 for MRI. Pan *et al*. developed multifunctional perfluorocarbon (PFC)-cored nanocarrier functionalized with the VCAM-1-targeting linker peptide, VLTTGLPALISWIKRKRQQ, for imaging in $ApoE^{-/-}$ mice.[41] The VCAM-1-targeted lipidic PFC NP showed a four-fold increase in accumulation in the aortas of $ApoE^{-/-}$ mice, resulting in enhanced ^{19}F MR contrast compared to the control (Figure 2).

Because MRI has shown promise in its superior capability of characterizing atherosclerotic plaques with high accuracy and reproducibility, efforts have been directed towards optimizing the delivery of contrast agents. For instance, Burtea *et al*. synthesized ultrasmall superparamagnetic iron oxide particles (USPIO), which were revealed to be strong MRI contrast agents, and functionalized with VCAM-1-binding cyclic heptapeptides (NNSKSHT motif)

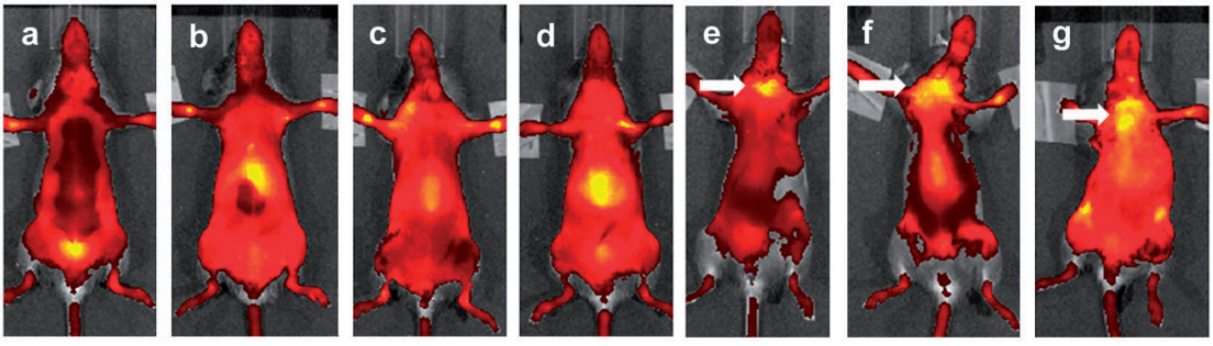

Figure 1 Cy7-labelled PAMs are detectable by near-IR *in vivo* imaging in $ApoE^{-/-}$ mice. (a) to (d) 24-h post injection, control (not functionalized with a targeting moiety) PAMs mostly show a strong signal in the bladder and liver, but not in the aorta. (e) to (g) In contrast, VCAM-1-targeting PAMs localize in the cardiovascular system (denoted by arrow), primarily in the aorta. Adapted from Mlinar *et al*.[40] with permission from Elsevier. (A color version of this figure is available in the online journal.)

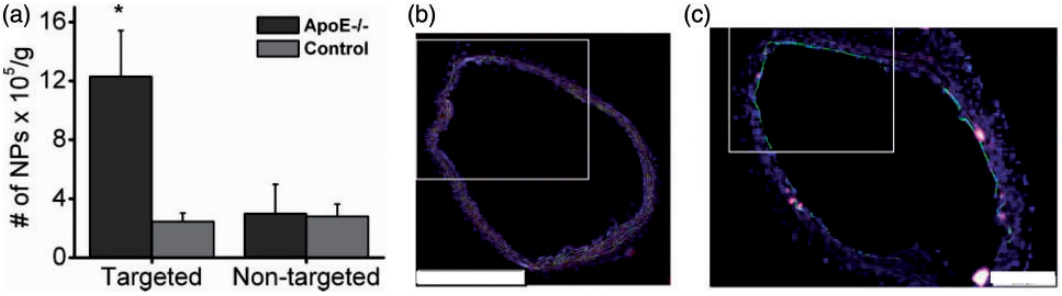

Figure 2 Multifunctional perfluorocarbon (PFC)-cored nanocarrier carrying VCAM-1-targeting linker peptide. (a) The VCAM-1-targeted NPs localized in the aortas of ApoE$^{-/-}$ mice, as signified by the higher ^{19}F signals compared to the control mice receiving targeted or non-targeted NPs and ApoE$^{-/-}$ mice receiving non-targeted nanoparticles. *$P < 0.05$. Histological analyses of *in vivo* targeting show that (b) only autofluorescence signals were detected in the aorta of control mice. Scale bar: 500 μm. (c) VCAM-1 staining (green) was strongly detected in the aorta of ApoE$^{-/-}$ mice (FITC-labeled secondary antibody). Blue is staining of cell nuclei by DAPI. Scale bar: 200 μm. Reprinted and adapted from Pan *et al*.[41] with permission from Federation of American Societies for Experimental Biology. (A color version of this figure is available in the online journal.)

for effective VCAM-1 targeting in aorta plaques.[42] The VCAM-1-targeting USPIO NPs were able to reach vulnerable plaques as quickly as 32 min post-injection compared to 221 min using the control, and at low doses of administration. This was further supported in a study by Michalska *et al*. in which the same cyclic heptapeptide was functionalized onto USPIO NPs to detect early and advanced atherosclerotic lesions.[43] By combining ultra-high-field MRI with surface-enhanced anti-Stokes Raman scattering microscopy, these USPIO NPs showed enhanced contrast, higher spatial resolution, and precise localizations in atherosclerotic lesions and cells expressing VCAM-1 within the vessel wall of ApoE$^{-/-}$ mice.

Regarding MRI, several NP-based platforms modified with chelated gadolinium (Gd), a contrast-enhancing agent, have been developed to target ECs and image atherosclerosis. Bruckman *et al*. synthesized VCAM-1 targeting, tobacco mosaic virus (TMV) NPs modified with sulfo-Cy5-azide dyes and Gd ions for dual optical-MR imaging capabilities *in vivo*.[44] Immunofluorescence imaging of aortas in ApoE$^{-/-}$ mice showed that the VCAM-1 targeting TMV NPs selectively localized to the activated ECs on atherosclerotic plaques compared to non-targeting control NPs. In addition, there was no accumulation of VCAM-1 targeting TMV NPs in healthy C57B1/6 mice. The authors hypothesized that the elongated shape of the NPs contributed to improved plaque localization, as more copies of the ligand could be presented to the flat vessel wall of atherosclerotic plaques compared to spherical NPs. Moreover, chelating Gd to TMV enabled plaque detection by MRI at an injected dose 400 times lower (0.00025 mmol/kg Gd ion) compared to the typical clinical dose of chelated Gd molecules (0.1 mmol/kg Gd ions). In a different study, Pagoto *et al*. developed phospholipid-based micelles containing the amphiphilic Gd-DOTAMA(C18)$_2$ and functionalized with the VCAM-1 receptor-targeting, cyclic peptide C*NNSKSHTC*C.[45] These Gd-based micelles demonstrated enhanced MRI T_1 signal (2–3-fold) in the inflamed region of lipopolysaccharide-induced mice compared to healthy and diseased mice administered free Gd, confirming successful targeting and increased contrast for inflammation detection.

In addition to diagnostics, advances have been made in the application of peptide-targeting NPs for therapeutic purposes in atherosclerosis. Kheirolomoom *et al*. developed a coated, cationic lipoparticle (CCL) nanocarrier carrying anti-miR-712 and VHP peptide (VHPK-CCL).[46] VHPK-CCLs selectively delivered anti-miR-712 to the pro-atherogenic, inflamed endothelium expressing VCAM-1 in disturbed-flow regions *in vivo*, while silencing miR-712 expression. As a result, VHPK-CCL-anti-miR-712 significantly reduced atherosclerotic lesions, ultimately inhibiting further disease progression. Furthermore, VHPK-CCL-anti-miR-712 could be injected at a dose 80% lower than that of naked anti-miR-712 to successfully prevent atheroma formation in ApoE$^{-/-}$ mice. Another peptide-therapeutic strategy by Calin *et al*. demonstrated the ability of PEGylated target-sensitive liposomes (TSL) carrying Teijin compound 1, an antagonist of the chemokine CCR2, to interfere with chemokine/receptor interaction at the surface of activated ECs.[47] The surface of the TSL was conjugated with VCAM-1 targeted peptide (VHPKQHRGGSKGC motif) to specifically bind to the developing atherosclerotic plaque in the aorta of ApoE$^{-/-}$ mice and deliver Teijin 1 compound to reduce monocyte infiltration and block inflammation. The effects of peptide-targeting were confirmed by fluorescent imaging, which revealed that non-targeted TSL had a 1.3-fold lower radiant efficiency compared to VCAM-1-targeting TSL.

Nanoparticles with the ability to co-deliver diagnostic and therapeutic agents on a single platform are termed ''theranostic'' NPs. These NPs offer benefits over NPs dedicated solely to diagnostics or therapeutics, as they can simultaneously treat the disease and monitor particle biodistribution in the body over time.[48] In this pursuit, Sun *et al*. developed self-assembling trifunctional Simian virus 40 (SV40) NPs encapsulated with quantum dots and the anticoagulant drug Hirulog and functionalized with a VCAM-1 targeting peptide (VHSPNKK motif) for targeting.[49] These multifunctional NPs were able to target, image, and deliver drugs to early, developmental, and late-stage atherosclerotic plaques in ApoE$^{-/-}$ mice. Selectively targeting VCAM-1 allowed a higher concentration of Hirulog to the sites of interest, confirming the ability of VHSPNKK to target VCAM-1. To overcome challenges of

optical imaging such as tissue absorbance and scattering, Sun *et al*. incorporated near-infrared quantum dots (NIR QDs) for their high detection sensitivity in deep-tissue imaging for early- and late-stage atherosclerosis in ApoE$^{-/-}$ mice. They demonstrated that the NIR QDs functionalized with the VCAM-1-targeting VHSPNKK peptide resulted in a 6.5-fold increase in accumulation to atherosclerotic plaques compared to QDs without the targeting moiety.

Ab-based nanomaterials for targeting VCAM in vivo

Functionalizing NPs with Abs is another common strategy used to enhance the diagnostic and therapeutic index at the diseased site while reducing off-target side effects. Abs, which are nanometer sized biological proteins part of the body's specific immune system, offer many advantages for *in vivo* imaging, targeting, and drug delivery in atherosclerosis.[50,51] For example, Abs allow NPs to bind to the target with enhanced affinity and increased cell penetration.[52] Like peptides, the small structure of antibodies allows for higher loading on the surfaces of NPs with limited steric constraints, substantially increasing the number of NPs that can be bound to the target.[53] Moreover, Abs enable NPs to be internalized via receptor-mediated endocytosis. These improvements in cellular uptake and intracellular stability allow for a higher intracellular concentration of drugs to be delivered at the intended site at or within the atherosclerotic plaque.

Tsourkas *et al*. developed magnetooptical NPs conjugated to anti-VCAM-1 Abs (VCAM-NP) to target and noninvasively image early-stage inflammation of the endothelium.[54] These VCAM-NPs were cross-linked with dextran-coated iron oxide, which has superparamagnetic properties, and Cy5.5 near-infrared fluorescent markers to enable detection by MRI and optical imaging. Following intravenous administration of VCAM-NPs to C57B1/6 mice, the fluorescent signal from NPs localizing to the activated EC surface signified selective targeting by the anti-VCAM-1 Abs.

Photoacoustic tomography (PAT) is another attractive imaging modality due to its nanomolar sensitivity to molecular contrast agents and sub-millimeter spatial resolution compared to MRI and fluorescence imaging. This is extremely important in the detection and characterization of atherosclerotic plaques and plaque progression, which require high spatial resolution and high molecular contrast to get an accurate prognosis and for subsequent therapy development. Gold nanoshells (AuNS) have strong absorption abilities and have been previously used for imaging applications in oncology, making these NPs an attractive molecular probe for imaging. Rouleau *et al*. synthesized gold nanoshell VCAM-1-targeted photoacoustic probes, known as immunonanoshells.[55] These immunonanoshells accumulated in VCAM-1 expressing atherosclerotic lesions of ApoE$^{-/-}$ mice by PAT. *Ex vivo* optical projection tomography of excised aorta confirmed this result, showing enhanced MR contrast.

Apart from optical imaging, MRI, and PAT, positron emission tomography-computed tomography (PET-CT) has been shown to have extremely high spatial resolution (3–5 nm), accurate quantification, and heightened sensitivity, making it a promising clinical imaging modality for atherosclerotic plaques detection. Bala *et al*. incorporated Fluorine-18 (^{18}F) on VCAM-1 nanobodies ([18F]FB-cABCAM-1-5), which are small antigen-binding fragments (12-15 kDa) from heavy-chain portion of Abs in camelids.[56] *In vivo* PET/CT imaging of ApoE$^{-/-}$ mice showed that cABCAM-1-5 were highly expressed in atherosclerotic lesions. *Ex vivo* analysis showed an increased uptake of targeted nanobodies in aortas 2.7 times higher than in control mice and 4.3 times higher compared to non-targeting nanobodies.

Modification of NPs with Abs to achieve therapeutic efficiency has also been accomplished. The anti-inflammatory properties of antiproliferative cyclopentenone prostaglandins (CP-PGs) make them optimal to incorporate in therapeutics against atherosclerosis. Antiproliferative cyclopentenone prostaglandins (CP-PGs) exhibit potent anti-inflammatory properties. Homen de Bittencourt *et al*. developed a negatively charged, liposome-based particle that was conjugated to anti-VCAM-1 Abs (LipoCardium) and was able to selectively deliver PGA2 to the injured arterial wall cells of adult LDL receptor knockout (ldlr$^{-/-}$) atherosclerotic mice.[57] At the site of inflammation, LipoCardium accumulated at the sites of adhesion molecules expressed on the inflamed EC surfaces and released PGA2 (Figure 3). It inhibited plaque progression through its tetravalent effects (anti-inflammatory, anti-inflammatory, anti-proliferative, anti-cholesterogenic, and cytoprotective), reversed vascular lesions, and reduced myocardium infractions in ldlr$^{-/-}$ mice compared to control non-treated ldlr$^{-/-}$ mice.

Targeting other CAMs in vivo

PECAM-1 and ICAM-1 are responsible for the transmigration of leukocytes from the blood vessel into the endothelium and intima.[30] PECAM-1- and ICAM-1-targeting platforms have also been developed to interfere with the inflammation of integrins and leukocytes responsible for endothelial monolayer integrity in various diseases. Although PECAM-1 and ICAM-1 have not been used directly in any *in vivo* NP applications for atherosclerosis, many researchers have used both of these targets to better understand their mechanistic and immunogenic properties. For example, Dziubla *et al*. developed a PECAM-targeted polymer nano-carrier (PNC) loaded with catalase enzyme to protect against vascular oxidative stress.[58] These PECAM-targeted nanocarriers demonstrated sufficient accumulation in the pulmonary vasculature, leading to reduced vascular oxidative stress. The authors theorized that this application could also be applied for atherosclerosis treatment. In another example, leukocyte-mimetic SPIO-based micelles (LMN) incorporated with LFA-1 integrin for ICAM-1 targeting demonstrated a rapid and noninvasive MR imaging technique to identify organ-specific inflammation in mice treated with lipopolysaccharides (LPS).[59] Due to the overexpression of ICAM-1 from LPS inflammation, there was a two-fold greater LMN accumulation in the liver of mice treated with LPS than that of

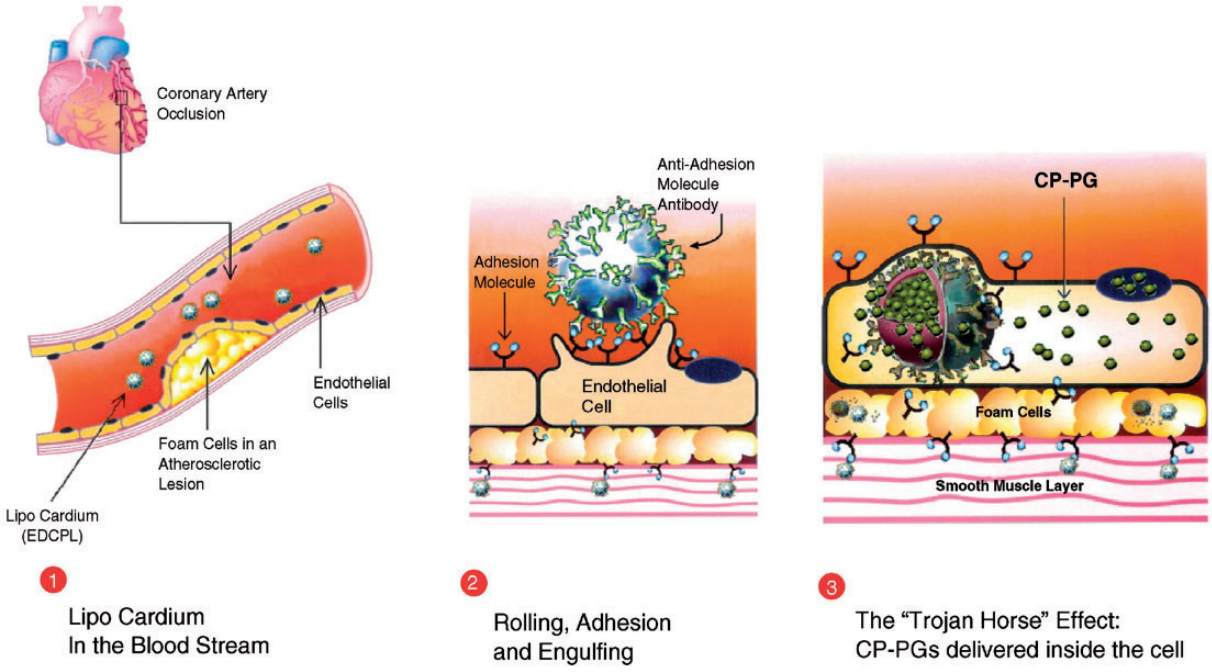

Figure 3 Endothelial dysfunction triggers inflammation, leading to an overexpression of VCAM-1 receptors on the surface of the activated ECs. (1) Following injection, the LipoCardium travel through the bloodstream. (2) The anti-VCAM-1 Abs lead the LipoCardium to VCAM-1 receptors, where it is taken up by the endothelial cell. (3) Once internalized by the cell, the lysosome disassembles and releases its contents, PGA2 molecules. Reprinted from Homem de Bittencourt *et al*.[57] with permission from Elsevier. (A color version of this figure is available in the online journal.)

non-ICAM-1 control mice. Serrano *et al*. demonstrated that the binding between ICAM-1 and ICAM-1 targeted carriers could induce CAM-mediated endocytosis.[60] The binding of these anti-ICAM carriers to ICAM-1 in the endothelium led to intracellular transport of these carriers by CAM-mediated endocytosis. The engagement of ICAM-1 in lipid domains, complexing with NHE1 (a linker between CAM-mediated endocytosis and cytoskeleton), acid shingomyelinase drives the hydrolysis of sphingomyelin into ceramide. The resulting actin polymerization and cytoskeleteon remodeling stabilizes the drug delivery platform and suggests that ECs can internalize relatively large drug carriers that are targeted to ICAM-1.

Flow-based *in vitro* models and CAMs expression

According to Zheng *et al*., the interplay between the arterial microenvironment and atherogenesis remains unclear, partially due to the gap between cell culture and animal experiments.[61] *In vitro* models can span the gap between 2D culture and *in vivo* testing, thus reducing the cost, time, and ethical burden of current approaches.[62] Furthermore, the lack of plaque rupture and thrombosis in animal models, gives advantage to *in vitro* systems for mimicking events that are characteristic of the late stages of the disease.[63] Studying endothelial mechanobiology requires engineered tools that can maintain EC in a controlled *in vitro* culture environment while exposing them to mechanical stimuli.[64]

Flow chamber-based models have been used to study both early- and late-stage pathogenic processes in atherosclerosis.[63] Various macro- and micro-scale cell culture flow (CCF) systems have been reviewed by Young and Simmons for studying adhesion, migration, flow-induced mechanotrasnduction, and permeability of ECs.[64] Cone-and-plate and parallel plate flow chamber (PPFC) are two most popular macro-scale CCF *in vitro* devices for controlled shear stress studies.[65] The family of CAMs are used for targeted delivery of drugs and imaging probes to the endothelium.[66,67] In this next section, we briefly review the *in vitro* flow models and their implementation with micro- and nanoparticles that have been specifically developed for: (1) studying the effect of disturbed flow on CAM expression and leukocyte recruitment and (2) evaluating the targeting efficiency to endothelium by using CAMs.

CAM expression, leukocyte recruitment, and disturbed flow

Leukocytes, including neutrophils and monocytes, adhere to the site of inflammation.[68,69] Tethering and rolling of leukocytes on ECs are controlled by selectins (E and P), adhesion is regulated by integrins, and transmigration is guided through the gap junctions by PECAM-1. Consequently, evaluating CAM expression in flow for ECs is central to understanding the nature of interaction of leukocytes with ECs. Initiation of atherosclerosis involves endothelial dysfunction in response to oxidative cholesterol particles as well as altered local hemodynamics.[63]

Disturbed and non-laminar flow below healthy physiological levels of shear stress (10–70 dyn/cm^2) can cause EC phenotype changes resulting in pro-inflammatory endothelium.[70–72] Here, we review *in vitro* models developed for determining the role of disturbed flow patterns on CAM expression and leukocyte recruitment, and conclude with the testing of targeted particles against CAMs in such models.

Cicha *et al*. studied adhesion of human monocyte cell-line (THP-1) at 5 dyn/cm^2 to HUVECs that have been perfused at 10 dyn/cm^2 for 18 h in a bifurcating flow-through cell (y-shaped μ-Slide).[73] Cells in the straight segment of the channel exposed to uniform shear stress had polygonal shape and elongated and aligned with the direction of the flow. On the contrary, cells exposed to non-uniform stress in bifurcations had irregular shapes. The authors observed an induction of E/P-selectins, VCAM-1, and ICAM-1 for the cells exposed to non-uniform shear stress compared to the cells in the straight segment. A moderate increase in the cells' ability to recruit monocytes was observed upon exposure to non-uniform shear stress.

Adhesion of neutrophils to human abdominal aortic endothelial cells (HAAEC) has been studied by Rouleau *et al*. in an eccentric stenosis model (divided into five sections: inlet, proximal, peak, recirculation and distal zones) with 50% area reduction (Figure 4(a)).[74] Acute promyelocytic leukemia cell line (NB4) activated with all-trans-retionic acid (ATRA) appeared to be significantly attached to the recirculation zone of the model for both the non-stimulated and TNF-α stimulated cells under stress conditions of 1.25 and 6.25 dyn/cm^2. Higher levels of VCAM-1 were detected near the stenosis peak of 1.25 dyn/cm^2. The adhesion was also dependent on time (1 vs. 6 h) and shear magnitude. Pre-shearing the cells at 1.25 dyn/cm^2 for 24 h significantly

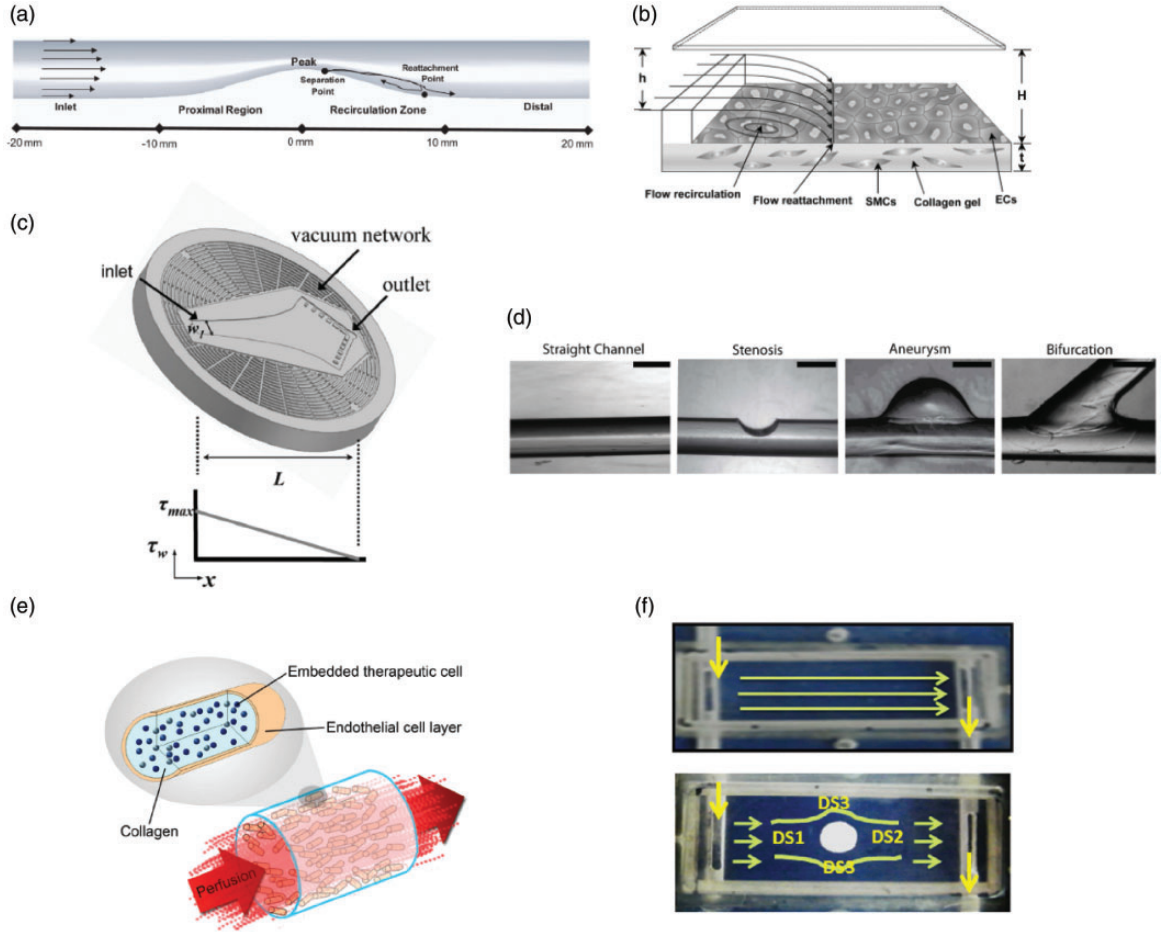

Figure 4 Various *in vitro* models for studying disturbed flow and CAM expression. (a) Asymmetric stenosis model. Model flow regions, including the inlet, proximal, peak, recirculation and distal regions. Adapted and reprinted from Rouleau *et al*.[74] with permission from the American Society of Hematology. (b) Schematic diagram of the flow channel and test section. Flow separation occurs in the region distal to the step, forming four specific flow areas. Adapted and reprinted from Chen *et al*.[75] with permission from IOP Publishing. (c) PDMS mold of the linear shear flow chamber and surrounding vacuum network that seals the chamber to the HAEC monolayer on a cover slip. Adapted and reprinted from Tsou *et al*.[77] with permission from the American Physiological Society. (d) Representative bright field images of multiple vascular geometries including a straight channel, stenosis, aneurysm, and bifurcation. Adapted and reprinted from Mannino *et al*.[80] with permission from Nature Publishing Group. (e) Modular, sub-millimeter-sized cylinders are made from collagen with embedded functional cells and surface-attached endothelial cells. Adapted and reprinted from Khan and Sefton[81] with permission from Elsevier. (f) The image on the top shows the view of laminar flow, and the image at the bottom shows the disturbed flow and regions selected for the study DS1, DS2, and DS3 based on the WSS measurement. Adapted and reprinted from Balaguru *et al*.[82] with permission from Nature Publishing Group. (A color version of this figure is available in the online journal.)

decreased the adhesion of NB4 cells (lasting 1 h) to both stimulated and non-stimulated ECs. Pre-shearing caused cells to express higher levels of ICAM-1 and VCAM-1 in the recirculation zone.

Chen *et al*. used a vertical step flow system (divided into four sections: stagnant flow area, recirculation eddy, reattachment area, and developed laminar flow) that exposed the cells to shear stresses (Figure 4(b)) in the range of 0–7 dyn/cm^2 and investigated the adhesion/transmigration of leukocytes in ECs co-cultured with smooth muscle cells (SMCs).[75] There was significant adhesion of neutrophils, lymphocytes, and monocytes to IL-1β activated co-culture system consisting of ECs seed on SMCs in the reattachment zone of this model. Co-culturing ECs with SMCs significantly amplified the adhesion of leukocytes relative to ECs cultured alone. Compared to neutrophils and lymphocytes, monocytes showed very low mobility underneath the ECs, suggesting that they possess the greatest likelihood to be deposited in the vessel wall following transmigration into the sub-endothelial space.

Conway *et al*. developed a PPFC reversing flow system to recreate the physiological form of the reversing shear stress (time-average: 1 dyn/cm^2, maximum 11 dyn/cm^2 and minimum of −11 dyn/cm^2) of the carotid sinus wall.[76] HUVECs exposed to high steady shear stress (15 dyn/cm^2) for 24 h aligned to the direction of flow, while cells exposed to low steady shear stress of 1 dyn/cm^2 or to the reversing flow were randomly oriented. Upon stopping the perfusion of THP-1 monocytes after 24 h, significant increase for adhesion was observed in the cells exposed to the reversing flow compared to static, low and high stress. Increasing values for ICAM-1 expression was observed for reversing flow compared to the static condition, while no increase for VCAM-1 expression could be detected.

In another study, Tsou *et al*. studied monocyte recruitment by TNF-α activated HAECs in a PDMS microfluidic flow chamber exposing the cells to a linear gradient of shear stress that increased from 0 to 16 dyn/cm^2 (Figure 4(c)).[77] Spatial variations of ICAM-1, VCAM-1, and E-selectin were determined and it was concluded that VCAM-1 expression is regulated with the highest spatial acuity in response to small fluctuations in shear stress. Furthermore, spatial CAM regulation is dependent on the magnitude of the applied stress and not the gradient. A specially designed configuration consisting of three independent rectangular flow channels allowed the authors to assess leukocyte recruitment at a constant shear rate (0, 2, 6, and 12 dyn/cm^2). Moreover, in separate experiments, the authors assessed monocyte rolling, arrest, and transmigration in the direction parallel to that of shear preconditioning. At a critical steady shear stress of 7 dyn/cm^2, CAM expression was altered and monocyte recruitment and arrest was significantly increased.

Reduced wall shear stress (WSS) that occurs following implementation of coronary stents favors restenosis due to an increase in neointimal proliferation.[78] Punchard *et al*.[79] evaluated the effect of stent deployment on HUVECs in a tubular flexible silicon model of artery fabricated by dip-coating a non-adherent mandrel. Stent deployment affected the local flow pattern and significantly reduced cell alignment. Alteration of expression of inflammation-associated genes was also measured. Upregulation of inflammatory gene expressions (E-selectin, ICAM-1, and VCAM-1) was found 24 h post stent deployment. Mannino *et al*. prepared different geometries (stenosis, aneurysm, and bifurcation) with PDMS channels of circular cross section (Figure 4(d)).[80] WSSs in different locations of multiple variations of these geometries were calculated using computational fluid dynamics (CFD). By varying the percent stenosis, aneurysm radius, and bifurcation angle in their ''do-it-yourself'' models, the wall shear stress could be varied at different locations in their model. The authors could demonstrate a correlation between WSS and VCAM-1 expression in these models.

Khan *et al*. created a modular tissue-engineered construct by randomly assembling HUVEC seeded collagen made modules in a PDMS microfluidic chamber to study the effect of disturbed flow on cell activation (Figure 4(e)).[81] Based on VCAM-1 and ICAM-1 expressions after 1 and 24 h of flow, no statistically significant up/downregulation was observed. Khan *et al*. also replicated the disturbed flow pattern of a modular tissue engineering construct in a microfluidic device exposing HUVEC cells to low (2.8 dyn/cm^2) and high (15.6 dyn/cm^2) average shear stress, where flow is in transitional state.[70] The PDMS microfluidic chamber was constructed by producing 3D images of packed modules using microcomputed tomography and then extracting a single plane image for photomask production. Perfusion of device with THP-1 cells confirmed that areas where multiple channels converge (node region of their model) are most prone to THP-1 attachment. Strong correlation between ICAM-1 and VCAM-1 expression was observed and high shear stress caused downregulation of activation markers.

Estrada *et al*. fabricated a microfluidic device capable of generating normal (average shear stress = 11 dyn/cm^2) and disturbed flow (average shear stress = 1.3 dyn/cm^2) patterns of atherosclerosis susceptible regions of abdominal aorta.[72] By exposing HAECs to these types of flow, the authors concluded that in the absence of pro-inflammatory stimulation, PECAM-1, VCAM-1, and ICAM-1 were not significantly upregulated by flow condition. Cells cultured under disturbed flow exhibited round shape and random orientation.

Balaguru and co-workers created disturbed flow by placing a circular block at the center of a PPFC seeded with human endothelial line (EAhy926) to create three regions (DS1, DS2, and DS3) with different flow characteristics around this block (Figure 4(f)).[82] Based on CFD analysis, lowest shear stress (5 dyn/cm^2) was experienced behind the block (DS2) where retrograde flow was present and cells maintained polygonal shape similar to that of static control. For this region, the authors observed a different pattern of actin compared to the other regions where actin fibers were seen at the periphery of the cells opposed to the centralized dispersive pattern. ICAM-1 and PECAM-1 gene expression levels were quantified in each region and were compared to normal shear stress setting where no block was present. Replacing the circular block with a different shape

(e.g. square, triangle, and irregular) is an interesting approach for studying real plaque mimicking conditions.

Targeting efficacy of particles to endothelium using CAMs

As stated by Kusunose *et al.*, having an effective model for quantifying particle binding under near *in vivo* conditions is crucial for development and optimization of targeted nanocarriers.[83] According to Muzykantov *et al.*, endothelial adhesion molecules are ideal markers for detection and drug delivery targets to treat vascular inflammation, thrombosis and oxidative stress.[66] We next turn our attention to the *in vitro* determination of binding and internalization of VCAM-1-, ICAM-1-, PECAM-1- and selectin-targeting particulate carriers under the action of a flow field.

VCAM-1. Yang *et al.* prepared VCAM-1 targeted core-shell Fe_3O_4@SiO_2 NPs (355 ± 37 nm) by reverse micro-emulsion.[84] They investigated adhesion of these particles to a monolayer of HUVECs in PPFS (shear stresses of 0, 1.1, 5.15, and 9.94 dyn/cm^2) upon stimulation with lipopolysaccharide (LPS) for 5 h for induction of inflammation. Adhesion of VCAM-1 targeted Fe_3O_4@SiO_2 particles was significantly higher when the cells were treated with LPS. The observed degree of adhesion decreased with increasing the shear stress and duration of exposure (0, 1, 5, and 10 min). Treatment of activated cells with anti-VCAM-1 Abs slightly decreased the binding of NPs which verified the VCAM-1 mediated adhesion of these particles. Kusunose *et al.* fabricated two different PDMS microfluidic chambers seeded with HUVEC to expose these cells to uniform (4.4 dyn/cm^2) and gradient shear stresses (2.4–8.6 dyn/cm^2).[83] Binding avidities of VHP peptide coated liposome were compared in static and dynamic conditions to TNF-α-activated HUVEC cells. Greatest accumulation for both 1% and 2% conjugated VHP liposomes occurred at the lowest shear rate and decreased steadily due to increased shear stress in the gradient shear chamber. In an uniform shear chamber, higher binding was observed by increasing the VHP peptide concentration in the liposomes while increasing the polyethylene-glycol (PEG) brush layer decreased the accumulation in both static and dynamic (4.4 dyn/cm^2) cultures (Figure 5(a)). Relative to static culture, liposome binding was significantly amplified upon the application of the uniform shear stress for 1% and 2% VHP-conjugated liposomes. Gosk *et al.* prepared immunoliposomes conjugated to VCAM-1 Abs (83.1 ± 14.4 nm).[85] Binding of these liposomes to murine brain endothlioma cells (bEnd.3) was assessed in a doublet flow chamber activated with TNF-α (4 h) at shear rates of about 200 s^{-1} (20 h). The authors determined that approximately 8% of the bound liposomes were internalized after 2 h. To confirm specificity, binding of VCAM-1 targeted liposomes was microscopically compared with human IgG conjugated liposomes of irrelevant specificity but similar size (91.3 ± 13.2 nm) over a period of 20 h.

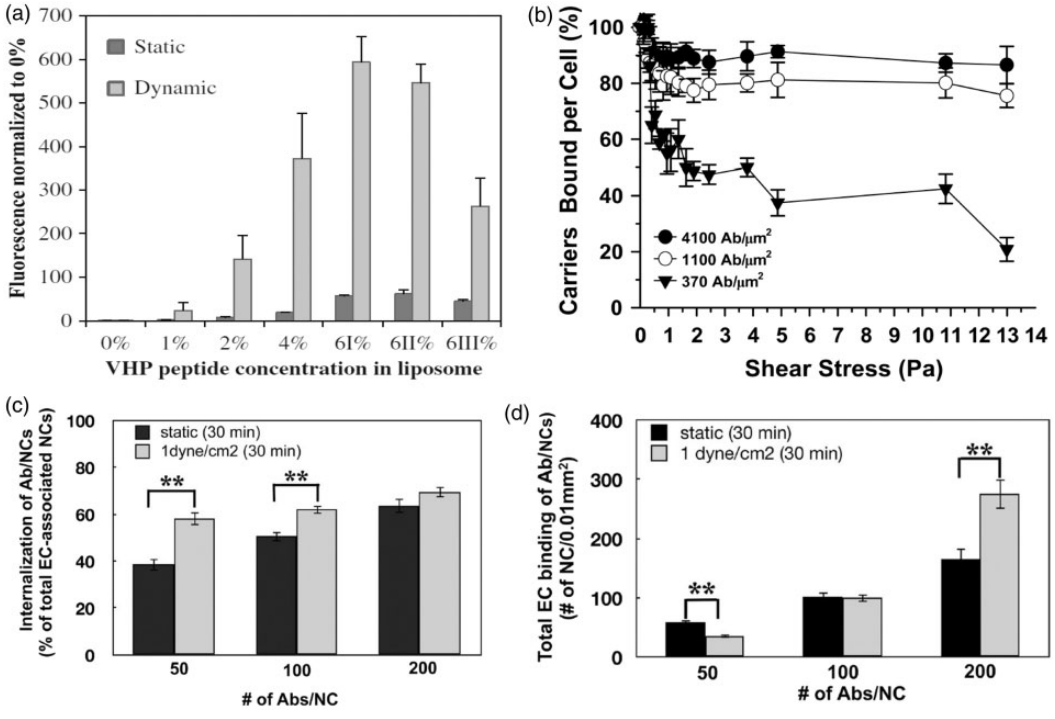

Figure 5 Effect of targeting ligand concentration on binding, internalization, and detachment of CAM targeted particles in flow. (a) VHP-conjugated liposome binding under static and shear conditions. Particle binding consistently increased with peptide concentration ($p < 0.01$), and also increased under shear ($p < 0.01$ except for 1%, up to 13-fold) ($n \geq 3$). Reprinted from Kusunose *et al.*[83] with permission from Biomedical Engineering Society. (b) Shear stress-induced detachment of anti-ICAM carriers from HUVEC. Data represent mean ± standard errors ($n = 30$ carriers). Reprinted from Calderon *et al.*[86] with permission from IOS press. Acute exposure to flow stimulates endocytosis of anti-PECAM/NCs in EC. Effect of flow (1 dyn/cm^2, 30 min) on endothelial internalization (c) and binding (d) of Abs/NC carrying 50, 100, and 200 Ab molecules per NC. Adapted from Han *et al.*[93] with permission from the American Chemical Society. (NC: nanocarrier)

ICAM-1. Calderon *et al*. investigated the dynamics of adhesion and detachment of 1 μm poly(styrene) (PS) beads coated with Abs against ICAM-1 to TNF-α activated human umbilical vein endothelial cells (HUVEC) using PPFC.[86] Fixing cells with paraformaldehyde allowed exclusive investigation of particle binding of without the interference of carrier internalization. Four distinct patterns for the carriers were observed: (1) no interaction, (2) continuous rolling, (3) first rolling and then binding, and (4) first rolling and then detachment. Increasing ICAM-1 surface density (370, 1100, 4100 molecules per μm^2) on the carrier resulted in a reduction in rolling velocity while increasing shear stress (0.1 and 0.5 Pa) amplifies this velocity. For the lowest Ab density tested (370 molecules per μm^2), the detachment of the particle was steep when increasing the shear stress (Figure 5(b)). However, higher Ab densities (1100 and 4100 molecules per μm^2) showed a markedly different behavior consisting of a minimal initial detachment and formation of a stable bond for the range of shear stresses explored (0–13 Pa). This study provided insight into monocyte attachment mechanisms for further investigation.

CAM-mediated endocytosis of NP in PPFC was explored by Bhowmick *et al*.[87] They determined the internalization of anti-ICAM Ab-coated PS particles (180 nm) in TNF-α activated flow-adapted (4 dyn/cm^2) HUVEC cells cultured in PPFC. Cells that adapted a 24-h flow internalized the particles at a slower rate compared to none flow-adapted cells. The effect of treatment of flow-adapted ECs with inhibitors of endocytic pathways was also investigated by these authors. Among the inhibitors tested, amiloride (which inhibits CAM endocytosis) showed the strongest inhibitory effect. Targeting efficiency of a multimodal N-succinimidyl S-acetylthioacetate (SATA) ICAM-1-conjugated liposomal contrast agent (163 ± 2 nm) to TNF-α activated ECs in a unidirectional flow system (μ-Slide) has been studied by Paulis *et al*.[88] Although higher levels of stress resulted in higher ICAM-1 expression, application of flow reduced the ability of the targeted liposomes to adhere to mouse endothelioma cells (bEnd.5) within the range of stresses studied (0, 0.25, and 0.5 Pa).

Rosano *et al*. fabricated a physiologically realistic polydimethylsiloxane (PDMS)-based synthetic microvascular network (SMN) from the mapped microvascular network of a hamster cremaster muscle using a modified Geographic Information Systems (GIS) approach.[89] Compared to control IgG conjugated spheres, a significantly larger number of mouse anti-ICAM-1-conjugated particles (2 μm PS spheres) adhered to the ECs using SMN seeded with bovine aortic endothelial cells (BAEC) and activated with TNF-α for 4 and 24 h. The effect of shape on targeting Ab-coated NPs to endothelium was investigated by Kolhar *et al*.[90] PS nanospheres (200 ± 0.01 nm in diameter) and nanorods (501 ± 43.6 nm × 123.6 ± 13.3 nm) of equal volume were coated with anti-ICAM-1 Abs for evaluating their endothelial targeting in a PDMS-based SMN seeded with rat brain endothelial cells (RBE4) activated with TNF-α. Greater attachment and internalization for nanorods was observed compared to anti-ICAM-1-coated nanospheres and IgG-coated spheres/rods flown at the shear rate of 240 s^{-1}. Muro *et al*.[91] conjugated anti-ICAM-1 molecules to PS spheres (7000 molecules per μm^2) and evaluated their targeting efficacy. PPFC seeded with HUVEC and activated with TNF-α at the shear stress of 9 dyn/cm^2 was used to determine the kinetics of NP binding under both static and flow conditions, which were both very rapid and indistinguishable from one another. The effect of exposure of HUVECs plated in PPFC to microparticles from human atherosclerotic plaques has been investigated by Rautou *et al*.[92] The authors measured the adhesion of human monocytic cells (U937) in low (1 dyn/cm^2) and high (10 dyn/cm^2) shear stress and concluded that the exposure of ECs to plaque MP favors monocytic cell adhesion by transferring ICAM-1 to ECs.

PECAM-1 and selectins. Han *et al*. studied binding and internalization of PS NPs coated with anti-PECAM-1 Abs (180–200 nm) to endothelium following exposure to chronic and acute shear stress.[93] A six-channel μ-Slide was used to subject HUVEC cells to laminar shear stresses. These authors demonstrated that following a 16-h exposure to chronic steady flow at 5 dyn/cm^2, endocytosis of the particles over a period of 30 min is diminished due to phenotype changes associated with flow adaptation, compared to non-flow-adapted cells. On the contrary, acute shear stress exposure (1 dyn/cm^2 for 30 min) increased the internalization of these NPs containing 50, 100, and 200 Ab molecule per particle (Figure 5(c)). When exposed to acute stress, binding of low avidity NPs (50 Ab molecules per particle) to endothelium was decreased, while for high avidity particles (200 Ab molecules per particle) the binding was increased compared to the static culture (Figure 5(d)). Maximal internalization for low avidity NPs was observed at shear stresses in the range of 2–4 dyn/cm^2 for the values explored at 0–8 dyn/cm^2. Charoenphol *et al*.[94] studied the targeting efficiency of PS particles coated (avidin-biotin) with silaly Lewis^a (sLe^a), selectins-specific ligand, to HUVECs using PPFC. For 10 μm particles, the highest binding was observed in the presence of red blood cells (RBC) in plasma flow at the WSR of 200 s^{-1} upon activation with IL-1β. At a fixed volume concentration, particle adhesion increased with an increase in size within the ranges (0.1, 0.5, 2, 5, and 10 μm) explored. These researches observed a critical WSR beyond which disruptive hemodynamic forces interfere with particle adhesion. The effect of channel height was also investigated by varying the height (127, 254, 508, 762 μm) at the WSR of 200 s^{-1}. For 2, 5, and 10 μm particles, an increase in channel height results in higher particle binding. No significant difference was observed for adhesion levels when comparing inverted channel to upright. A significant difference in binding was only seen with 5 and 10 μm particles at low channel heights and WSR in the inverted chamber.

The effect of particle shape on adhesion of sLe^a coated PS particles was investigated by Thompson *et al*.[95] HUVECs in PPFC were activated with IL-1β and targeting efficacy was evaluated in reconstituted blood using steady and pulsatile flow profiles. Three sets of particles with equivalent

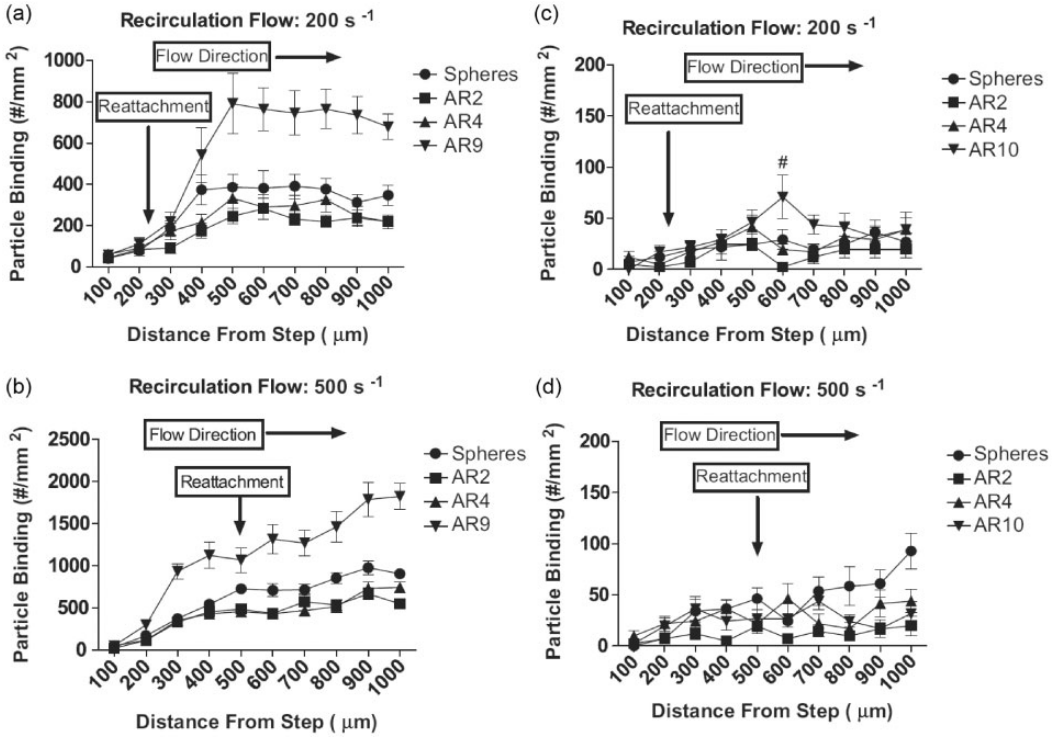

Figure 6 Role of aspect ratio (AR) on binding of targeted particles in various locations of the step channel geometry. Adhesion of spheres and rods with 2 μm ESD [(a) 200 s^{-1}, (b) 500 s^{-1}] and 500 nm ESD [(c) 200 s^{-1}, (d) 500 s^{-1}] to activated ECs from 40% RBC in buffer at a fixed particle concentration of 5×10^5 #/mL. Reprinted from Thompson *et al*.[95] with permission from Elsevier

spherical diameters (ESD) of 2.07, 1.01, and 0.52 μm were used where the aspect ratio (AR) varied in each set. Increasing WSR did not result in a significant difference in the adhesion of any particles for the smallest ESD. For particle shapes with ESD of 2 μm, increasing WSR resulted in a decrease in normalized binding efficiency of particles with ARs of 1, 2, and 4, while for rods with AR of 9, high binding efficiency was observed for all the shear rates tested (200, 500, and 1000 s^{-1}). In pulsatile flow, highest binding was observed for 2 μm particles with ARs of 9 to 11. Moreover, the adhesion of these particles in various locations of the step channel geometry was measured. Far downstream from the stagnation point, the adhesion of particles with AR of 9 and ESD of 2 μm was highest at the WSR of 200 and 500 s^{-1} (Figure 6(a) and (b) correspondingly) Interestingly, for WSR of 200 s^{-1}, at the stagnation point of the step channel, particle adhesion did not show any shape or AR dependency. For ESD of 0.5 μm, no improvement in adhesion due to particle shape or WSR was detected in the step channel and adhesion was minimal (Figure 6c and Figure 6d). Lin *et al*. prepared PS NPs (100 nm) conjugated to glycocalicin (the extracellular segment of platelet glycoprotein Ibα that specifically binds to P-selectin) using avidin-biotin complex.[96] The authors investigated the effect of shear stress on uptake of these NPs by histamine-activated human aortic endothelial cells (HAECs) exposed to 0, 5, and 15 dyn/cm^2 of shear stress in a PPFC. Increasing shear stress drastically decreased the uptake of non-conjugated NPs, but not for glycocalicin conjugated particles.

Conclusion

A variety of peptides and Abs have been utilized *in vivo* to target the characteristic overexpressed CAMs in atherosclerosis. This gives researchers a wide selection of potential designs when developing diagnostic or therapeutic strategies. For instance, the development of molecular, contrast agents for MRI has been a large focus of current imaging research using nanomedicine that can translate into the clinic.[45] Therapies that seek out sites of CAM do not rely on traditional symptoms of atherosclerosis such as unnatural levels of lipoproteins, high blood pressure, and body weight, but are able to directly deliver drugs to the plaque site and even reverse vascular lesions based on molecular and cellular markers of the disease.[58] Many CAM-targeting particles (Table 2) have been tested *in vitro* in microfluidic devices and parallel-plate flow chambers that are able to elucidate atherogenic physical stimuli. As such, patterns of disturbed flow[70] and wall shear stresses[82] and their relation to CAM expression can set the stage for yet undiscovered *in vitro* devices. As CVD is expected to remain a priority health issue, the rapid pace of advances in NP theranostics is sure to continue. As *in vitro* models move to those of greater complexity and physiological relevance with the use of sophisticated and advanced technologies including 3D printing and complex co-culture conditions, the multifaceted parameters of atherosclerosis can be further replicated. Current and upcoming *in vivo* and *in vitro* studies will allow the testing of novel therapeutics in a timely and cost-effective manner for the atherosclerosis.

Table 2 Various synthetic CAM targeting particles tested *in vitro* by different researchers using flow-based models

Targets	Targeting moieties	Particle types	*In vitro* models	References
VCAM-1	VHPKQHR Peptide	Liposome	PDMS Microfluidic	83
	Phycoerythrin-labeled Ab	Core-Shell Fe_3O_4@SiO_2	PPFC	84
	Ab(MK271)	Liposome	Doublet Flow Chamber	85
ICAM-1	Ab(R6.5)	PS Latex Particles	PPFC	86
	Ab(R6.5)	PS Spheres	PPFC	87
	Ab(YN1/1.7.4)	Liposome	μ-Slide (Ibidi, Germany)	88
	Ab	PS Spheres	PDMS Microvascular Networks	89
	Ab	PS Nanospheres/Nanorods	PDMS Microfluidic Networks	90
	Ab(R6.5)	PS Spheres	PPFC	91
PECAM-1	Ab(Ab62)	PS Spheres	μ-Slide (Ibidi, Germany)	93
Selectin-E	sLe[a]	PS Spheres	PPFC	94
	sLe[a]	PS Spheres/Rods	PPFC	95
Selectin-P	Glycocalicin	Carboxylated PS Spheres	PPFC	96

Note: The corresponding Ab clones are indicated in the parentheses.

Authors' contribution: KK, JJML and CP contributed equally. KK, CP, and EJC conceived the concept. KK, JJML, CP, JW, and EJC wrote the review.

ACKNOWLEDGEMENTS

The authors thank Manjima Sarkar for her helpful discussions. The authors would like to acknowledge the financial support from the University of Southern California and the National Heart, Lung, and Blood Institute (NHLBI) (grant no. R00HL124279).

DECLARATION OF CONFLICTING INTERESTS

The author(s) declared no potential conflicts of interest with respect to the research, authorship, and/or publication of this article.

REFERENCES

1. Mozaffarian D, Benjamin EJ, Go AS, Arnett DK, Blaha MJ, Cushman M, Das SR, de Ferranti S, Després J-P, Fullerton HJ, Howard VJ, Huffman MD, Isasi CR, Jiménez MC, Judd SE, Kissela BM, Lichtman JH, Lisabeth LD, Liu S, Mackey RH, Magid DJ, McGuire DK, MOhler ER, Moy CS, Muntner P, Mussolino ME, Nasir K, Neumar RW, Nichol G, Palaniappann L, Pandey DK, Reeves MJ, Rodriguez CJ, Rosamond W, Sorlie PD, Stein J, Towfighi A, Turan TN, Virani SS, Woo D, Yeh RW, Turner MB. Heart disease and stroke statistics-2016 update: a report from the American Heart Association. *Circulation* 2016;**133**:e38–60
2. National Institutes of Health National Heart L, and Blood Institute. *NHLBI Fact Book*, Fiscal year 2012, http://www.nhlbi.nih.gov/about/documents/factbook/2012 (accessed 31 October 2016)
3. Falk E. Pathogenesis of atherosclerosis. *J Am Coll Cardiol* 2006;**47**:C7–12
4. Rahmani M, Cruz RP, Granville DJ, McManus BM. Allograft vasculopathy versus atherosclerosis. *Circ Res* 2006;**99**:801–15
5. Galkina E, Ley K. Immune and inflammatory mechanisms of atherosclerosis. *Annu Rev Immunol* 2009;**27**:165–97
6. van der Wal AC, Becker AE. Atherosclerotic plaque rupture - pathologic basis of plaque stability and instability. *Cardiovasc Res* 1999;**41**:334–44
7. Singh RB, Mengi SA, Xu Y-J, Arneja AS, Dhalla NS. Pathogenesis of atherosclerosis: a multifactorial process. *Exp Clin Cardiol* 2002;**7**:40–53
8. Berliner JA, Navab M, Fogelman AM, Frank JS, Demer LL, Edwards PA, Watson AD, Lusis AJ. Atherosclerosis: basic mechanisms. Oxidation, inflammation, and genetics. *Circulation* 1995;**91**:2488–96
9. Doran AC, Meller N, McNamara CA. Role of smooth muscle cells in the initiation and early progression of atherosclerosis. *Arterioscler, Thromb, Vasc Biol* 2008;**28**:812–9
10. Swirski FK, Weissleder R, Pittet MJ. Heterogeneous in vivo behavior of monocyte subsets in atherosclerosis. *Arterioscler, Thromb, Vasc Biol* 2009;**29**:1424–32
11. Tzima E, Irani-Tehrani M, Kiosses WB, Dejana E, Schultz DA, Engelhardt B, Cao G, DeLisser H, Schwartz MA. A mechanosensory complex that mediates the endothelial cell response to fluid shear stress. *Nature* 2005;**437**:426–31
12. Yavuz MS, Cheng Y, Chen J, Cobley CM, Zhang Q, Rycenga M, Xie J, Kim C, Song KH, Schwartz AG, Wang LV, Xia Y. Gold nanocages covered by smart polymers for controlled release with near-infrared light. *Nat Mater* 2009;**8**:935–9
13. Lee JE, Lee N, Kim H, Kim J, Choi SH, Kim JH, Kim T, Song IC, Park SP, Moon WK, Hyeon T. Uniform mesoporous dye-doped silica nanoparticles decorated with multiple magnetite nanocrystals for simultaneous enhanced magnetic resonance imaging, fluorescence imaging, and drug delivery. *J Am Chem Soc* 2010;**132**:552–7
14. Sajja HK, East MP, Mao H, Wang YA, Nie S, Yang L. Development of multifunctional nanoparticles for targeted drug delivery and noninvasive imaging of therapeutic effect. *Curr Drug Discov Technol* 2009;**6**:43–51
15. Cheon J, Lee J-H. Synergistically integrated nanoparticles as multimodal probes for nanobiotechnology. *Acc Chem Res* 2008;**41**:1630–40
16. Rieter WJ, Pott KM, Taylor KML, Lin W. Nanoscale coordination polymers for platinum-based anticancer drug delivery. *J Am Chem Soc* 2008;**130**:11584–5
17. Peer D, Karp JM, Hong S, Farokhzad OC, Margalit R, Langer R. Nanocarriers as an emerging platform for cancer therapy. *Nat Nanotechnol* 2007;**2**:751–60
18. Li S-D, Huang L. Pharmacokinetics and biodistribution of nanoparticles. *Mol Pharm* 2008;**5**:496–504
19. Kim KS, Khang G, Lee D. Application of nanomedicine in cardiovascular diseases and stroke. *Curr Pharm Des* 2011;**17**:1825–33
20. Karagkiozaki V, Logothetidis S, Pappa A-M. Nanomedicine for atherosclerosis: molecular imaging and treatment. *J Biomed Nanotechnol* 2015;**11**:191–210

21. Schiener M, Hossann M, Viola JR, Ortega-Gomez A, Weber C, Lauber K, Soehnlein O. Nanomedicine-based strategies for treatment of atherosclerosis. *Trends Mol Med* 2014;**20**:271–81
22. Chung EJ, Tirrell M. Recent advances in targeted, self-assembling nanoparticles to address vascular damage due to atherosclerosis. *Adv Healthcare Mater* 2015;**4**:2408–22
23. Fang J, Nakamura H, Maeda H. The EPR effect: unique features of tumor blood vessels for drug delivery, factors involved, and limitations and augmentation of the effect. *Adv Drug Deliv Rev* 2011;**63**:136–51
24. Knop K, Hoogenboom R, Dagmer F, Schubert U. Poly(ethylene glycol) in drug delivery: Pros and cons as well as potential alternatives. *Angew Chem Int Ed* 2010;**49**:6288–308
25. Yu MK, Park J, Jon S. Targeting strategies for multifunctional nanoparticles in cancer imaging and therapy. *Theranostics* 2012;**2**:3–44
26. Deshpande PP, Biswas S, Torchilin VP. Current trends in the use of liposomes for tumor targeting. *Nanomedicine* 2013;**8**:1509–28
27. Danhier F, Feron O, Preat V. To exploit the tumor microenvironment: Passive and active tumor targeting of nanocarriers for anti-cancer drug delivery. *J Control Release* 2010;**148**:135–46
28. Devalapally H, Chakilam A, Amiji MM. Role of nanotechnology in pharmaceutical product development. *J Pharm Sci* 2007;**96**:2547–65
29. Haley B, Frenkel E. Nanoparticles for drug delivery in cancer treatment. *Urol Oncol: Semin Orig Invest* 2008;**26**:57–64
30. Galkina E, Ley K. Vascular adhesion molecules in atherosclerosis. *Arterioscler Thromb Vasc Biol* 2007;**27**:2292–301
31. Ley K, Huo Y. VCAM-1 is critical in atherosclerosis. *J Clin Invest* 2001;**107**:1209–10
32. Blankenberg S, Barbaux S, Tiret L. Adhesion molecules and atherosclerosis. *Atherosclerosis* 2003;**170**:191–203
33. Chia MC. The role of adhesion molecules in atherosclerosis. *Crit Rev Clin Lab Sci* 1998;**35**:573–602
34. Woodfin A, Voisin M-B, Nourshargh S. PECAM-1: A multi-functional molecule in inflammation and vascular biology. *Arterioscler Thromb Vasc Biol* 2007;**27**:2514–23
35. Nakashima Y, Raines EW, Plump AS, Breslow JL, Ross R. Upregulation of VCAM-1 and ICAM-1 at atherosclerosis-prone sites on the endothelium in the apoE-deficient mouse. *Arterioscler Thromb Vasc Biol* 1998;**18**:842–51
36. Chung EJ. Targeting and therapeutic peptides in nanomedicine for atherosclerosis. *Exp Biol Med* 2016;**241**:891–8
37. Acar H, Srivastava S, Chung EJ, Schnorenberg MR, Barrett JC, LaBelle JL, Tirrell M. Self-assembling peptide-based building blocks in medical applications. *Adv Drug Delivery Rev*2016; Epub ahead of print 14 August. DOI: 10.1016/j.addr.2016.08.006
38. Kelly KA, Allport JR, Tsourkas A, Shinde-Patil VR, Josephson L, Weissleder R. Detection of vascular adhesion molecule-1 expression using a novel multimodal nanoparticle. *Circ Res* 2005;**96**:327–36
39. Nahrendorf M, Jaffer FA, Kelly KA, Sosnovik DE, Aikawa E, Libby P, Weissleder R. Noninvasive vascular cell adhesion molecule-1 imaging identifies inflammatory activation of cells in atherosclerosis. *Circulation* 2006;**114**:1504–11
40. Mlinar LB, Chung EJ, Wonder EA, Tirrell M. Active targeting of early and mid-stage atherosclerotic plaques using self-assembled peptide amphiphile micelles. *Biomaterials* 2014;**35**:8678–86
41. Pan H, Myerson JW, Hu L, Marsh JN, Hou K, Scott MJ, Allen JS, Hu G, San roman S, Lanza GM, Schreiber RD, Schlesinger PH, Wickline SA. Programmable nanoparticle functionalization for in vivo targeting. *FASEB J* 2013;**27**:255–64
42. Burtea C, Ballet S, Laurent S, Rousseaux O, Dencausse A, Gonzalez W, Port M, Corot C, Vander Elst L, Muller RN. Development of a magnetic resonance imaging protocol for the characterization of atherosclerotic plaque by using vascular cell adhesion molecule-1 and apoptosis-targeted ultrasmall superparamagnetic iron oxide derivatives. *Arterioscler Thromb Vasc Biol* 2012;**32**:e36–e48
43. Michalska M, Machtoub L, Manthey HD, Bauer E, Herold V, Krohne G, Lykowsky G, Hildenbrand M, Kampf T, Jakob P, Zernecke A, Bauer WR. Visualization of vascular inflammation in the atherosclerotic mouse by ultrasmall superparamagnetic iron oxide vascular cell adhesion molecule-1-specific nanoparticles. *Arterioscler Thromb Vasc Biol* 2012;**32**:2350–7
44. Bruckman MA, Jiang K, Simpson EJ, Randolph LN, Luyt LG, Yu X, Steinmetz NF. Dual-modal magnetic resonance and fluorescence imaging of atherosclerotic plaques in vivo using VCAM-1 targeted tobacco mosaic virus. *Nano Lett* 2014;**14**:1551–8
45. Pagoto A, Stefania R, Garello F, Arena F, Digilio G, Aime S, Terreno E. Paramagnetic phospholipid-based micelles targeting VCAM-1 receptors for MRI visualization of inflammation. *Bioconjugate Chem* 2016;**27**:1921–30
46. Kheirolomoom A, Kim CW, Seo JW, Kumar S, Son DJ, Gagnon MK, Ingham ES, Ferrara KW, Jo H. Multifunctional nanoparticles facilitate molecular targeting and miRNA delivery to inhibit atherosclerosis in apoE$^{-/-}$ mice. *ACS Nano* 2015;**9**:8885–97
47. Calin M, Stan D, Schlesinger M, Simion V, Deleanu M, Constantinescu CA, Gan AM, Pirvulescu MM, Butoi E, Manduteanu I, Bota M, Enachescu M, Borsig L, Bendas G, Simionescu M. VCAM-1 directed target-sensitive liposomes carrying CCR2 antagonists bind to activated endothelium and reduce adhesion and transmigration of monocytes. *Eur J Pharm Biopharm* 2015;**89**:18–29
48. Xie J, Lee S, Chen X. Nanoparticle-based theranostic agents. *Adv Drug Delivery Rev* 2010;**62**:1064–79
49. Sun X, Li W, Zhang X, Qi M, Zhang Z, Zhang X-E, Cui Z. In vivo targeting and imaging of atherosclerosis using multifunctional virus-like particles of simian virus 40. *Nano Lett* 2016;**16**:6164–71
50. Arruebo M, Valladares M, Gonzalez-Fernandez A. Antibody-conjugated nanoparticles for biomedical applications. *J Nanomater* 2009;**2009**:24
51. Binder CJ, Silverman GJ. Natural antibodies and the autoimmunity of atherosclerosis. *Springer Semin Immunopathol* 2005;**26**:385–404
52. Cardoso MM, Peca IN, Roque ACA. Antibody-conjugated nanoparticles for therapeutic applications. *Curr Med Chem* 2012;**19**:3103–27
53. McCarthy JR, Weissleder R. Multifunctional magnetic nanoparticles for targeted imaging and therapy. *Adv Drug Deliv Rev* 2008;**60**:1241–51
54. Tsourkas A, Shinde-Patil VR, Kelly KA, Patel P, Wolley A, Allport JR, Weissleder R. In Vivo imaging of activated endothelium using an anti-VCAM-1 magnetooptical probe. *Bioconjugate Chem* 2005;**16**:576–81
55. Rouleau L, Berti R, Ng VWK, Matteau-Pelletier C, Lam T, Saboural P, Kakkar AK, Lesage F, Rhéaume E, Tardif JC. VCAM-1-targeting gold nanoshell probe for photoacoustic imaging of atherosclerotic plaque in mice. *Contrast Media Mol Imag* 2013;**8**:27–39
56. Bala G, Blykers A, Xavier C, Descamps B, Broisat A, Ghezzi C, Fagret D, Van Camp G, Caveliers V, Vanhove C, Lahoutte T, Droogmans S, Cosyns B, Devoogdt N, Hernot S. Targeting of vascular cell adhesion molecule-1 by 18F-labelled nanobodies for PET/CT imaging of inflamed atherosclerotic plaques. *Eur Heart J Cardiovasc Imag* 2016;**17**:1001–8
57. Homem de Bittencourt PI, Lagranha DJ, Maslinkiewicz A, Senna SM, Tavares AMV, Baldissera LP, Janner DR, Peralta JS, Bock PM, Gutierrez LL, Scola G, Heck TG, Krause MS, Cruz LA, Abdalla DS, Lagranha CJ, Lima T, Curi R. LipoCardium: Endothelium-directed cyclopentenone prostaglandin-based liposome formulation that completely reverses atherosclerotic lesions. *Atherosclerosis* 2007;**193**:245–58
58. Dziubla TD, Shuvaev VV, Hong NK, Hawkins BJ, Madesh M, Takano H, Simone E, Nakada MT, Fisher A, Albelda SM, Muzykantov VR. Endothelial targeting of semi-permeable polymer nanocarriers for enzyme therapies. *Biomaterials* 2007;**29**:215–27
59. Wong R, Chen X, Wang Y, Hu X, Jin MM. Visualizing and quantifying acute inflammation using ICAM-1 specific nanoparticles and MRI quantitative susceptibility mapping. *Ann Biomed Eng* 2012;**40**:1328–38
60. Serrano D, Bhowmick T, Chadha R, Garnacho C, Muro S. Intercellular adhesion molecule 1 engagement modulates sphingomyelinase and ceramide, supporting uptake of drug carriers by the vascular endothelium. *Arterioscler Thromb Vasc Biol* 2012;**32**:1178–85
61. Zheng W, Huang R, Jiang B, Zhao Y, Zhang W, Jiang X. An early-stage atherosclerosis research model based on microfluidics. *Small* 2016;**12**:2022–34

62. Ryan AJ, Brougham CM, Garciarena CD, Kerrigan SW, O'Brien FJ. Towards 3D in vitro models for the study of cardiovascular tissues and disease. *Drug Discov Today* 2016;**21**:1437–45
63. Benam KH, Dauth S, Hassell B, Herland A, Jain A, Jang K-J, Karalis K, Kim HJ, MacQueen L, Mahmoodian R, Musah S, Torisawa YS, van der Meer AD, Villenave R, Yadid M, Parker KK, Ingber DE. Engineered In vitro disease models. *Annu Rev Pathol Mech Dis* 2015;**10**:195–262
64. Young EWK, Simmons CA. Macro- and microscale fluid flow systems for endothelial cell biology. *Lab Chip* 2010;**10**:143–60
65. Rezvan A, Ni C-W, Alberts-Grill N, Jo H. Animal, in vitro, and ex vivo models of flow-dependent atherosclerosis: Role of oxidative stress. *Antioid Redox Signal* 2011;**15**:1433–48
66. Muzykantov VR. Targeted drug delivery to endothelial adhesion molecules. *ISRN Vasc Med* 2013;**2013**:27
67. Chacko A-M, Hood ED, Zern BJ, Muzykantov VR. Targeted nanocarriers for imaging and therapy of vascular inflammation. *Curr Opin Colloid* 2011;**16**:215–27
68. Cooper S, Emmott A, Jonak P, Rouleau L, Leask RL. In vitro leukocyte adhesion in endothelial tissue culture models under flow. In: Dhanjoo N, Ghista (eds). *Biomedical science, engineering and technology*. Rijeka, Croatia: InTech, 2012, pp. 191–208. Available at: http://www.intechopen.com/books/biomedical-science-engineering-and-technology/in-vitro-leukocyte-adhesion-in-endothelial-tissue-culture-models-under-flow (accessed 6 February 2017)
69. Chung EJ, Mlinar LB, Nord K, Sugimoto MJ, Wonder E, Alenghat FJ, Fang Y, Tirrell M. Monocyte-targeting supramolecular micellar assemblies: a molecular diagnostic tool for atherosclerosis. *Adv Healthcare Mater* 2015;**4**:367–76
70. Khan OF, Sefton MV. Endothelial cell behaviour within a microfluidic mimic of the flow channels of a modular tissue engineered construct. *Biomed Microdevices* 2011;**13**:69–87
71. Chiu J-J, Usami S, Chien S. Vascular endothelial responses to disturbed flow: pathologic implications for atherosclerosis. In: Artmann GM, Chien S (eds). *Bioengineering in Cell and Tissue Research*. New York: Springer, 2008, pp. 469–96
72. Estrada R, Giridharan GA, Nguyen M-D, Prabhu SD, Sethu P. Microfluidic endothelial cell culture model to replicate disturbed flow conditions seen in atherosclerosis susceptible regions. *Biomicrofluidics* 2011;**5**:032006–11
73. Cicha I, Margarete G-S, Yilmaz A, Daniel WG, Garlichs CD. Endothelial dysfunction and monocyte recruitment in cells exposed to non-uniform shear stress. *Clin Hemorheol Microcirc* 2008;**39**:113–9
74. Rouleau L, Copland IB, Tardif J-C, Mongrain R, Leask RL. Neutrophil adhesion on endothelial cells in a novel asymmetric stenosis model: effect of wall shear stress gradients. *Ann Biomed Eng* 2010;**38**:2791–804
75. Chen C-N, Chang S-F, Lee P-L, Chang K, Chen L-J, Usami S, Chien S, Chiu JJ. Neutrophils, lymphocytes, and monocytes exhibit diverse behaviors in transendothelial and subendothelial migrations under coculture with smooth muscle cells in disturbed flow. *Blood* 2006;**107**:1933–42
76. Conway DE, Williams MR, Eskin SG, McIntire LV. Endothelial cell responses to atheroprone flow are driven by two separate flow components: low time-average shear stress and fluid flow reversal. *Am J Physiol Heart Circ Physiol* 2010;**298**:H367–74
77. Tsou JK, Gower RM, Ting HJ, Schaff UY, Insana MF, Passerini AG, Simon SI. Spatial regulation of inflammation by human aortic endothelial cells in a linear gradient of shear stress. *Microcirculation* 2008;**15**:311–23
78. Mongrain R, Rodes-Cabau J. Role of shear stress in atherosclerosis and restenosis after coronary stent implantation. *Rev Esp Cardiol* 2006;**59**:1–4
79. Punchard MA, O'Cearbhaill ED, Mackle JN, McHugh PE, Smith TJ, Stenson-Cox C, Barron V. Evaluation of human endothelial cells post stent deployment in a cardiovascular simulator in vitro. *Ann Biomed Eng* 2009;**37**:1322–30
80. Mannino RG, Myers DR, Ahn B, Wang Y, Margo R, Gole H, Lin AS, Guldberg RE, Giddens DP, Timmins LH, Lam WA. Do-it-yourself in vitro vasculature that recapitulates in vivo geometries for investigating endothelial-blood cell interactions. *Sci Rep* 2015;**5**:12401
81. Khan OF, Sefton MV. Perfusion and characterization of an endothelial cell-seeded modular tissue engineered construct formed in a microfluidic remodeling chamber. *Biomaterials* 2010;**31**:8254–61
82. Balaguru UM, Sundaresan L, Manivannan J, Majunathan R, Mani K, Swaminathan A, Venkatesan S, Kasiviswanathan D, Chatterjee S. Disturbed flow mediated modulation of shear forces on endothelial plane: a proposed model for studying endothelium around atherosclerotic plaques. *Sci Rep* 2016;**6**:27304
83. Kusunose J, Zhang H, Gagnon MKJ, Pan T, Simon SI, Ferrara KW. Microfluidic system for facilitated quantification of nanoparticle accumulation to cells under laminar flow. *Ann Biomed Eng* 2013;**41**:89–99
84. Yang H, Zhao F, Li Y, Xu M, Li L, Wu C, Miyoshi H, Liu Y. VCAM-1-targeted core/shell nanoparticles for selective adhesion and delivery to endothelial cells with lipopolysaccharide-induced inflammation under shear flow and cellular magnetic resonance imaging in vitro. *Int J Nanomedicine* 2013;**8**:1897–906
85. Gosk S, Moos T, Gottstein C, Bendas G. VCAM-1 directed immunoliposomes selectively target tumor vasculature in vivo. *Biochim Biophys* 2008;**1778**:854–63
86. Calderon AJ, Muzykantov V, Muro S, Eckmann DM. Flow dynamics, binding and detachment of spherical carriers targeted to ICAM-1 on endothelial cells. *Biorheology* 2009;**46**:323–41
87. Bhowmick T, Berk E, Cui X, Muzykantov VR, Muro S. Effect of flow on endothelial endocytosis of nanocarriers targeted to ICAM-1. *J Control Release* 2012;**157**:485–92
88. Paulis LE, Jacobs I, van den Akker NM, Geelen T, Molin DG, Starmans LW, Nicolay K, Strijkers GJ. Targeting of ICAM-1 on vascular endothelium under static and shear stress conditions using a liposomal Gd-based MRI contrast agent. *J Nanobiotechnol* 2012;**10**:25
89. Rosano JM, Tousi N, Scott RC, Krynska B, Rizzo V, Prabhakarpandian B, Pant K, Sundaram S, Kiani MF. A physiologically realistic in vitro model of microvascular networks. *Biomed Microdevice* 2009;**10**:1007/s10544–009-9322-8
90. Kolhar P, Anselmo AC, Gupta V, Pant K, Prabhakarpandian B, Ruoslahti E, Mitragotri S. Using shape effects to target antibody-coated nanoparticles to lung and brain endothelium. *Proc Natl Acad Sci USA* 2013;**110**:10753–8
91. Muro S, Dziubla T, Qiu W, Leferovich J, Cui X, Berk E, Muzykantov VR. Endothelial targeting of high-affinity multivalent polymer nanocarriers directed to intercellular adhesion molecule 1. *J Pharm Exp Ther* 2006;**317**:1161
92. Rautou P-E, Leroyer AS, Ramkhelawon B, Devue C, Duflaut D, Vion A-C, Nalbone G, Castier Y, Leseche G, Lehoux S, Tedgui A, Boulanger CM. Microparticles from human atherosclerotic plaques promote endothelial ICAM-1–dependent monocyte adhesion and transendothelial migration". *Circ Res* 2011;**108**:335–43
93. Han J, Zern BJ, Shuvaev VV, Davies PF, Muro S, Muzykantov V. Acute and chronic shear stress differently regulate endothelial internalization of nanocarriers targeted to platelet-endothelial cell adhesion molecule-1. *ACS Nano* 2012;**6**:8824–36
94. Charoenphol P, Huang RB, Eniola-Adefeso O. Potential role of size and hemodynamics in the efficacy of vascular-targeted spherical drug carriers. *Biomaterials* 2010;**31**:1392–402
95. Thompson AJ, Mastria EM, Eniola-Adefeso O. The margination propensity of ellipsoidal micro/nanoparticles to the endothelium in human blood flow. *Biomaterials* 2013;**34**:5863–71
96. Lin A, Sabnis A, Kona S, Nattama S, Patel H, Dong JF, Nguyen KT. Shear-regulated uptake of nanoparticles by endothelial cells and development of endothelial-targeting nanoparticles. *J Biomed Mater Res A* 2010;**93A**:833–42